The phonon spectra and elastic constants of Pd_xFe_{1-x}: an understanding from inter-atomic interactions

2009 J. Phys.: Condens. Matter 21 095411

(http://iopscience.iop.org/0953-8984/21/9/095411)

J. Phys.: Condens. Matter **21** (2009) 095411 (9pp) doi:10.1088/0953-8984/21/9/095411

The phonon spectra and elastic constants of Pd_xFe_{1-x}: an understanding from inter-atomic interactions

Biswanath Dutta and Subhradip Ghosh

Department of Physics, Indian Institute of Technology Guwahati, Guwahati, Assam 781039, India

E-mail: subhra@iitg.ernet.in

Received 18 October 2008, in final form 20 January 2009
Published 9 February 2009
Online at stacks.iop.org/JPhysCM/21/095411

Abstract

Understanding the role of the inter-atomic force constants in lattice dynamics of random binary alloys is a challenging problem. Addressing these inter-atomic interactions accurately is a necessity to obtain an accurate phonon spectrum and to calculate properties from them. Using a combination of *ab initio* density functional perturbation theory (DFPT) and the itinerant coherent potential approximation (ICPA), an analytic, self-consistent method for performing configuration averaging in random alloys, we model the inter-atomic force constants for $Pd_{0.96}Fe_{0.04}$ and $Pd_{0.9}Fe_{0.1}$ alloys based upon the *ab initio* results and intuitive arguments. The calculated phonon dispersion curves and elastic constants agree very well with the experimental results. Comparison of our results with those obtained in a model potential scheme is also done. The modeling of inter-atomic interactions in random alloys and their roles regarding the phonon-related properties are also discussed in light of these results.

1. Introduction

The calculation and analysis of phonon excitations in ordered intermetallics and disordered alloys is one of the fundamental areas in materials science research. The energy dispersion of phonons provides rich information about the dynamical properties of the material [1]. In particular, it is an essential input in the calculation of thermodynamic properties like the heat capacities, thermal expansion coefficients, transport properties like diffusivity and quantities like the electron–phonon interactions, to name just a few. More recently, the analysis of phonon spectra of materials has been extremely useful in studying the contribution of vibrational entropy towards phase stability and phase transition at finite temperature. A wealth of experimental data on a variety of intermetallics and substitutionally disordered alloys is now available [2–5]. The experimental data include disordered alloys at both stoichiometric and off-stoichiometric compositions. The experimental analysis mostly dealt with the calculation of vibrational entropy in a given phase or the calculation of the difference in vibrational entropy between phases, calculation of migration enthalpy or vacancy formation enthalpy due to diffusion because of technological relevance. For these analyses, the average vibrational density of states is the only quantity required. However, to understand the underlying microscopic nature of the complex interplay of forces between various pairs of species in an alloy, detailed information on the phonon dispersion and the force constant data is necessary. The dispersion curves though can be obtained from experiments but the force constants are obtained simply by fitting experimental frequencies to simple Born–Von Karman models. This approach works for ordered alloys but fails to exhibit the variation of force constants between various species in a completely random environment. On the theoretical side, the calculation of the full phonon dispersion, the force constants and the densities of states have been made possible due to the advent of first-principles calculations. As a result, the experimental data can be successfully interpreted for ordered alloys. Compared to this, a suitable theoretical approach to study the disordered phases, in particular, for off-stoichiometric compositions is yet lacking. The additional complexities in substitutionally disordered systems are the finite phonon lifetimes, a quantity which is far more sensitive than the dispersion curves or the densities of states. There have been numerous investigations on the phonon excitations in substitutionally disordered alloys at various concentrations

since the early 1960s to the late 1980s [6–10] but a complete understanding of the lattice dynamics has not been possible due to the lack of a suitable theory which can address all three important disorder effects: the mass disorder, the force constant disorder and the environmental disorder. The coherent potential approximation (CPA) [11] was the most successful theoretical tool to study disordered alloys and enforce the all important configuration averaging, but it had limited success for phonon excitations due to its single-site nature. Unlike the electronic excitations, the phonons have the off-diagonal disorder embedded in them because of the acoustic sum rule. A single-site theory cannot therefore address any kind of off-diagonal disorder. Successive cluster generalizations of the CPA [12–18] were either restrictive or non-analytic, and therefore unable to provide the solution. Recently, one of us successfully formulated a cluster generalization of the CPA which has the necessary analytic properties and is self-consistent [19]. This method, known as the 'itinerant coherent potential approximation' (ICPA), was able to calculate the phonon spectra and disorder-induced widths in different alloys [19–21]. However, the key input that needs to be fed into this Green's function-based method for performing configuration averaging of physical quantities is the inter-atomic force constant between various pairs of species. In [19–21], these force constants were either chosen empirically or were taken from the experiments, depending upon the physical reality in which comparisons between theory and experiments were being attempted. One, therefore, needs to look for better alternatives regarding the inter-atomic force constants in random alloys.

An understanding of the behavior of various inter-atomic force constants in a random environment is a necessity to analyze the phonon spectra and related properties, as has been demonstrated earlier [19]. This necessity is probably more in the case of the so-called type-II alloys where the constituents making up the alloy themselves crystallize in different structures in their elemental phases while a single unique lattice is formed upon alloying. Examples of such systems are iron–nickel, iron–platinum and iron–palladium. In disordered phases of these alloys, a unique fcc solid solution is formed whereas iron stabilizes in the bcc phase at room temperature. It is a well-known fact that FCC iron is unstable until one attains very high temperature [22]; the force constants in FCC iron at low temperatures are, therefore, expected to be soft. It would, therefore, be interesting to investigate the changes in the inter-atomic force constants associated with iron atoms, if any, and their impact on the phonon spectra in the disordered phases of a type-II alloy. We have chosen the Pd_xFe_{1-x} alloy for such an investigation. To our knowledge, such a systematic study on the behavior of the inter-atomic force constants and their role on the features of the phonon dispersion relations has not been done for this alloy. Neutron scattering experimental results on phonon frequencies and elastic constants are available for $x = 0.96$ and 0.9 [23] in this alloy. The only theoretical results available on these systems are based on a pair-potential method [24], later modified to include three-body interactions [25, 26]. In this approach, the model potential is generated from the dissociation energy of a pair of atoms, the distance between them and by fitting to the elastic constants. The three-body term is later evaluated by fitting the total interaction energy of an atom in a particular crystal structure to the total cohesive energy of the element. The inter-atomic force constants are then obtained from the spatial derivatives of these potentials. In the case of $Pd_{0.96}Fe_{0.04}$ and $Pd_{0.9}Fe_{0.1}$ the phonon spectrum obtained from the pair-potential-only model showed significant deviation from experiments and the elastic constants were off by about 25% on average. Although inclusion of the three-body term in the potential improved the phonon frequencies for these alloys, one serious drawback of the model potential approach is that the role of the electronic structure of the elements forming the alloy was altogether neglected. Since the inter-atomic interactions were dependent solely upon a given crystal structure and not on the electronic structure, the nearest-neighbor Fe–Fe and Pd–Pd inter-atomic force constants came out to be of the same order of magnitude (since the nearest-neighbor force constants in a FCC structure are an order of magnitude higher than the distant neighbors, we focus on these only). This result is completely counterintuitive because Fe–Fe force constants are expected to be softer than those for Pd–Pd for the reason mentioned above. The inter-atomic force constants as obtained by the model potential approach, therefore, seem not to represent the actual microscopic picture.

In this paper, we investigate the interrelations between the inter-atomic force constants and the lattice dynamics of $Pd_{0.96}Fe_{0.04}$ and $Pd_{0.9}Fe_{0.1}$. In this context, we present an alternative approach to calculate the inter-atomic force constants in these two alloys. This approach is a combination of an *ab initio* method which computes inter-atomic interactions based upon the detailed electronic structures and the itinerant coherent potential approximation which does the desired averaging over various configurations in the disordered alloy, addressing both mass as well as force constant disorder. We present results on phonon frequencies and elastic constants for these two alloys. Significant insight about the inter-atomic interactions between various pairs of chemical species is obtained in the course of our investigations. The role of the inter-atomic interactions in influencing the phonon spectra and the limitations of the model potential approach are also discussed in detail.

This paper is organized as follows. In section 2 we describe in some detail the various components of our methodology. Calculation details are presented in section 3. The results and discussions are presented in section 4. Concluding remarks and future directions are presented in section 5.

2. Methodology

2.1. Modeling the inter-atomic force constants

As has been discussed in section 1, the most crucial component in obtaining an accurate phonon spectrum and related properties in random alloys is the accurate modeling of the force constants. The best source for obtaining the inter-atomic force constants between a given pair of species

constituting the alloy is *ab initio* calculations which are parameter-free. However, no *ab initio* method for computing the inter-atomic force constants in a random alloy environment is yet available. Previously, a few attempts were made to obtain force constants for random alloys from *ab initio* calculations on a single ordered structure having the same symmetry as that of the alloy [20, 21]. Although the calculations are less expensive computationally, the results obtained were far from reality. An alternative approach was provided by Cedar and co-workers [27, 28]. In this approach, they found that the relevant force constants are strongly correlated with the bond lengths between a given pair of atoms and, as a result, the force constant versus bond length relationship is transferable across the compositions for a given alloy. The advantage of this approach is that the force constant versus bond length relationship can be obtained from a few first-principles calculations on select configurations and then can be transferred to determine force constants for other atomic configurations, once the relevant bond lengths are known. Although this approach is based upon a relatively simple idea, its implementation can be quite cumbersome when the alloy compositions deviate significantly from stoichiometric ones. The selected configurations for obtaining the force constant versus bond length relationships can themselves be quite complicated and therefore the calculations can be computationally expensive [29]. However, taking a cue from their observation that the force constants are dependent upon the bond distances, we here model the inter-atomic force constants for Pd_xFe_{1-x} alloys for $x = 0.96$ and 0.9 the following way: the Pd–Pd and Fe–Fe force constants are computed from *ab initio* calculations on pure FCC Fe and pure FCC Pd at the lattice constants of the random alloy. The reason behind this is twofold; first, the size difference between Fe and Pd atoms is not appreciable. Therefore, there would not be appreciable dispersion of bond distances for Fe–Fe and Pd–Pd pairs. As a result, the FCC environment around each Fe and Pd atom in the original random alloy and the bond distances can be well represented by the calculations as outlined above; second, our results would be compared to those obtained from the model potential calculations to investigate and understand the complex interplay of interactions between various pairs of chemical species. Since the force constants generated from the model potentials were obtained at the alloy lattice constants, a direct comparison could be effected with this choice.

Modeling the Fe–Pd interactions is, however, tricky. In the model potential approach, the Fe–Pd force constants were considered to be simple concentration averages of the Fe–Fe and Pd–Pd force constants. We have tested the validity of this approach and our observations and further developments have been discussed in detail in section 4. We have used the density functional perturbation theory (DFPT) [30] for performing the *ab initio* calculations and the itinerant coherent potential approximation (ICPA) [19] for performing the configuration averaging. In the next two subsections, we briefly describe the features of these methods.

2.2. Density functional perturbation theory

Density functional perturbation theory (DFPT) is a density functional theory (DFT) [31, 32] based linear response method to obtain the electronic and lattice dynamical properties in condensed matter systems. The inter-atomic force constants required to calculate the phonon frequencies are derived via the linear response of the electronic subsystems [33]. The Hellmann–Feynman theorem [34, 35] is used to calculate the elements of the force constant matrices:

$$C_{\mathbf{R}_I\mathbf{R}_J} = \frac{-\partial \mathbf{F}_I}{\partial \mathbf{R}_J} = \int \frac{\partial n_{\mathbf{R}}(\mathbf{r})}{\partial \mathbf{R}_J}\frac{\partial V_{\mathbf{R}}(\mathbf{r})}{\partial \mathbf{R}_I}\,\mathrm{d}\mathbf{r} + \int n_{\mathbf{R}}(\mathbf{r})\frac{\partial^2 V_{\mathbf{R}}(\mathbf{r})}{\partial \mathbf{R}_I \partial \mathbf{R}_J} + \frac{\partial^2 E_N(\mathbf{R})}{\partial \mathbf{R}_I \partial \mathbf{R}_J} \quad (1)$$

$\mathbf{R}_I, \mathbf{R}_J$ are the ionic positions, $\mathbf{F}_I$ is the Hellmann–Feynman force on the Ith nucleus, $n_{\mathbf{R}}(\mathbf{r})$ is the ground state electronic charge density corresponding to the nuclear configuration $\mathbf{R}$, $V_{\mathbf{R}}(\mathbf{r})$ is the electron–nucleus interaction and E_N is the ion–ion interaction energy.

From equation (1) it is clear that the inter-atomic force constants are determined from the ground state charge density and from its linear response to a distortion in the ionic configuration. In the DFPT, these quantities are calculated within the DFT framework with a workload of the same order as that required for a standard ground state total energy calculation.

2.3. Itinerant coherent potential approximation

Based upon the *augmented space formalism* [36], a clever bookkeeping technique to account for disorder fluctuations in a random alloy environment, the itinerant coherent potential approximation (ICPA) is a mean-field based cluster generalization of the single-site coherent potential approximation (CPA) [11]. It is an analytic, self-consistent method of configuration averaging which preserves site-translational invariance. In this formalism, the coherent potential like the mean-field approximation begins with a *partition* of the augmented space into a part which is spanned by the *reference* or *null cardinality* state $|\{\emptyset\}\rangle$, the *average* configuration state and the remaining part $\mathbf{\Psi} - |\{\emptyset\}\rangle\langle\{\emptyset\}|$ spanned by the *fluctuation* states: $\{|\{C\}\rangle\}$. With this partition, any operator can be written in a block representation:

$$\mathbf{A} = \begin{pmatrix} \mathbf{A}_1 & \mathbf{A}' \\ \mathbf{A}'^{\dagger} & \mathbf{A}_2 \end{pmatrix}.$$

The partition or down-folding theorem then allows us to invert this operator in the subspace spanned by the *average* configurations alone. According to the augmented space theorem this is the configuration average of the quantity represented by $\mathbf{A}$. Defining the operator $\mathbf{K}$ as $(\mathbf{m}\omega^2\text{–}\mathbf{\Phi})$, $\mathbf{m}$ and $\mathbf{\Phi}$ being the mass and the force constant operators, respectively, and using the above partition: $\mathbf{K}_1 = (\langle\langle\mathbf{m}\rangle\rangle\omega^2 - \langle\langle\mathbf{\Phi}\rangle\rangle)$. The down-folding theorem and augmented space theorem together give us

$$\langle\langle\mathbf{G}(\omega^2)\rangle\rangle = (\mathbf{K}_1 - \mathbf{K}'^{\dagger}\mathbf{F}\mathbf{K}')^{-P_1}, = (\mathbf{G}^{-1}_{\mathrm{VCA}}(\omega^2) - \mathbf{\Sigma}(\omega^2))^{-P_1},$$

$$\mathbf{F} = \mathbf{K}_2^{-P_2} \quad \text{is the itinerator} \tag{2}$$

$$\mathbf{\Sigma} = \mathbf{K}'^{\dagger}\mathbf{F}\mathbf{K}' \quad \text{is the self-energy.} \tag{3}$$

Here $\mathbf{A}^{-P_1}$ and $\mathbf{A}^{-P_2}$ refer to the inverses of the operator $\mathbf{A}$ in the subspaces labeled by 1 and 2. Confining only to the *single fluctuation* states of the type $|\{R\}\rangle$ the self-energy is then computed self-consistently in this approximation. Adopting the notation $\langle\{R\}|\mathbf{A}|\{R'\}\rangle = A^{(R)(R')}$, and using the translational invariance of the augmented space operators, the self-energy and the *itinerator* $\mathbf{F}$ within the single fluctuation states can be approximated as

$$\mathbf{\Sigma} = \sum_{RR'} \mathbf{K}'^{\dagger(R)}\mathbf{F}^{(R)(R')}\mathbf{K}'^{(R')}, \tag{4}$$

$$\mathbf{F}^{(R)(R')} = \mathbf{G}^{(R)}\left[\delta_{RR'} + \sum_{R''} \mathbf{V}^{(R)(R'')}F^{(R'')(R')}\right]. \tag{5}$$

In going from equation (2) to (4) all contributions to the self-energy of configuration states with more than one fluctuation in more than one site have been neglected. Similarly, in going from equation (3) to (5), matrix elements of the itinerator $\mathbf{F}$ between configuration states with more than one fluctuation present at a time, which corresponds to coherent scattering from more than one site, have been neglected and such states do not contribute to $\mathbf{F}$ and hence to the self-energy $\mathbf{\Sigma}$ within this approximation. The second equation is a Dyson equation within the subspace spanned by only single fluctuation states. Self-consistency is achieved through

$$\mathbf{G}^{(R)} = \left(\mathbf{G}_{\mathrm{VCA}}^{-1} - \mathbf{\Sigma}^{(R)}\right)^{-1},$$

$$\mathbf{\Sigma}^{(R)} = \sum_{R'R''\neq R} \mathbf{K}'^{(R')}\mathbf{F}^{(R')(R'')}\mathbf{K}'^{(R'')}.$$

The above argument shows that, unlike the usual CPA where only a single fluctuation at a site is considered, multiple fluctuations coming from multiple scattering is present in the itinerator $\mathbf{F}$ and therefore contribute to the self-energy $\mathbf{\Sigma}$. In the context of phonon excitations, this enables one to use this formalism to accommodate the force constant disorder along with mass disorder.

3. Computational details

First-principles Quantum-Espresso code[1], based upon a plane wave-pseudopotential implementation of the DFPT, has been used to compute the Fe–Fe and Pd–Pd force constants at the alloy lattice parameters, 7.31 au for $Pd_{90}Fe_{10}$ and 7.339 au for $Pd_{96}Fe_4$. Ultrasoft pseudopotentials [37] with nonlinear core corrections [38] were used. Perdew–Zunger parameterization of the local density approximation [39] was used for the exchange–correlation part of the potential. Computation of the Fe–Fe force constants was also done with the PBE-96 GGA [40] exchange–correlation functional for the sake of comparison as there are serious doubts regarding the reliability of LDA results for iron. Plane waves with energies up to 55 Ryd are used in order to describe electron wavefunctions and Fourier components of the augmented charge density with cutoff energy up to 650 Ryd are taken into account. The Brillouin zone integrations are carried out with Methfessel–Paxton smearing [41] using a $12 \times 12 \times 12$ **k**-point mesh. The value of the smearing parameter is 0.02 Ryd. These parameters are found to yield phonon frequencies converged to within 5%.

After achieving the desired level of convergence for the electronic structure, the force constants are conveniently computed in reciprocal space on a finite **q**-point grid and Fourier transformation is employed to obtain the real-space force constants. The number of unique real-spaced force constants and their accuracy depend upon the density of the **q**-point grids: the closer the **q**-points are spaced, the more accurate the force constants are. In this work, we have used a $4 \times 4 \times 4$ **q**-point mesh.

The ICPA calculations were done on 400 energy points. The disorder in the force constants was considered for the nearest-neighboring shell only. A small imaginary frequency part of -0.05 was used in the Green's functions. The Brillouin-zone integration was done over 356 **q**-points in the irreducible Brillouin zone. The simplest linear-mixing scheme was used to accelerate the convergence. The number of iterations ranged from 5 to 15 for all the calculations.

4. Results

In the calculations of the phonon spectrum using the model pair potentials, the system was considered to be mean crystal-like where the mass was considered to be a concentration average of Fe and Pd masses and the force constant disorder was substantially weak. The weak force constant disorder resulted from the fact that the Fe–Fe and Pd–Pd force constants were of nearly the same magnitude and the Fe–Pd force constants were concentration averages of the above two. The Fe and Pd masses have a ratio ∼1:2; therefore the mass disorder in the alloy should be significant, apart from the force constant disorder. Clearly, a mean crystal model like the one followed in [24] and [25] would not work properly. To demonstrate this, we have done ICPA calculations with this set of force constants [24, 25] and with the masses of the constituents being kept equal to the concentration averaged mass. The results for $Pd_{0.9}Fe_{0.1}$ are presented in figure 1. The dispersion curves deviate substantially from the experimental results. The disagreement is greater as one goes towards the zone boundary. The agreement is near perfect for the longer wavelengths. The reason behind such discrepancies can be understood as follows: in the longer wavelength limit, self-averaging of both mass and force constants over a single wavelength reduces the ICPA to that of a mean crystal model like the virtual crystal approximation (VCA), making near perfect agreement with the experiments in our case; in the shorter wavelength regime where frequencies are higher the mass and the force constant disorders play a more significant role. In the mean crystal-like model generated by the model potential, all three inter-atomic force constants are pure Pd-like and the mass is an average

[1] Quantum-Espresso is a community project for high-quality quantum-simulation software, based on density functional theory, and coordinated by Paolo Gianozzi. See http://www.Quantum-Espresso.org/ and http://www.pwscf.org.

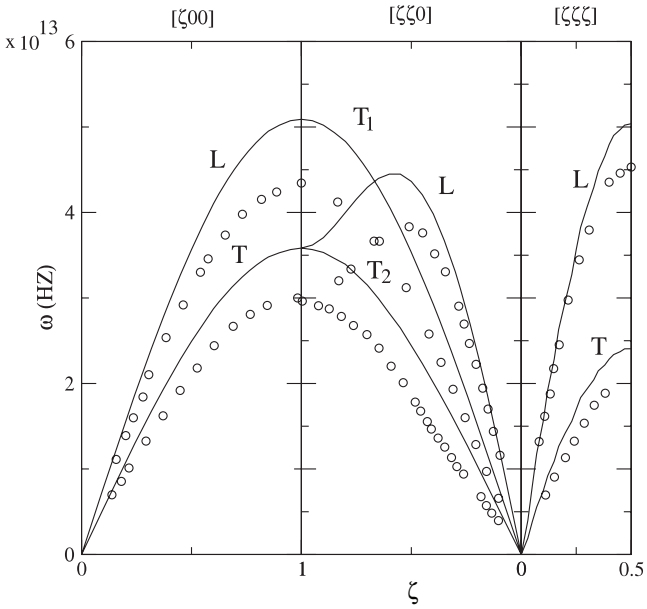

Figure 1. Dispersion curves (frequency ω versus reduced wavevector ζ); $\zeta = \frac{|\vec{q}|}{|\vec{q}_{\max}|}$, $\vec{q}$ the phonon wavevector; for $Pd_{0.9}Fe_{0.1}$ calculated in the ICPA (solid lines) with the force constants obtained from model potential. The circles are the experimental data.

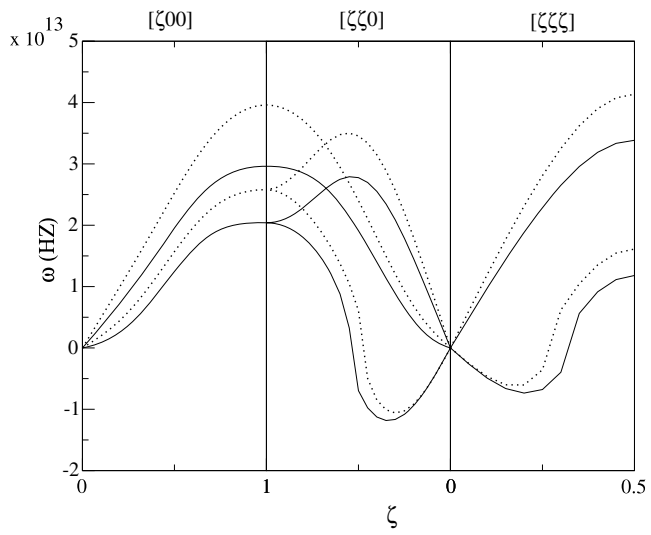

Figure 2. Calculated LDA (solid lines) and GGA (dotted lines) phonon dispersion curves of Fe in the FCC phase, both computed at the experimental lattice constant of $Pd_{0.90}Fe_{0.1}$.

Table 1. Computed force constants (in units of dyn cm^{-1}) for Pd_xFe_{1-x}. Fe–Fe and Pd–Pd force constants are obtained from DFPT calculations. Fe–Pd (averaged) force constants are the ones obtained by performing concentration averages on Fe–Fe and Pd–Pd force constants. Fe–Pd (reduced) force constants are the ones reduced by 20% from the Fe–Pd (averaged) values. L and T represent the longitudinal and the transverse force constants, respectively.

Pair type	Conc. (x)	L	T
Fe–Fe	0.96	13 366	−566
Pd–Pd	0.96	45 925	−2424
Fe–Pd (averaged)	0.96	44 623	−2349
Fe–Pd (reduced)	0.96	35 698	−1880
Fe–Fe	0.90	14 495	−609
Pd–Pd	0.90	48 768	−2699
Fe–Pd (averaged)	0.90	45 340	−2490
Fe–Pd (reduced)	0.90	36 272	−1992

one which is lower than that of the Pd mass. The phonon frequencies obtained, therefore, are overestimated as the mean crystal is like that of pure Pd with a reduced mass due to neglect of mass and force constant fluctuations.

In order to address the microscopic picture of inter-atomic interactions more realistically, we first focus on the lattice dynamics of FCC Fe at the lattice constants of the alloys considered. The dispersion curves of pure Fe calculated by the *ab initio* DFPT at the alloy lattice constant of $Pd_{0.9}Fe_{0.1}$ are presented in figure 2. The results with both the LDA exchange–correlation and with the GGA exchange–correlation are presented for the sake of comparison because the LDA is known to fail in reproducing the correct magnetic ground state of bcc iron [42]. The results show that the FCC Fe is dynamically unstable at the given lattice constant. This qualitative feature is identical for both exchange–correlation functionals. Quantitatively, the GGA frequencies are larger than those of the LDA. Since our only aim was to show that the dynamical instability of the Fe at the FCC phase and at the given lattice constant is independent of the exchange–correlation functional, the quantitative values of the phonon frequencies are irrelevant for the discussion. The results clearly demonstrate that the use of the LDA exchange–correlation functional is justified in the present case. The reason LDA works in the present case, although it even fails to produce the ferromagnetic ground state for the bcc structure, is the following: here we have done computations on the ferromagnetic-FCC phase of iron and at a lattice constant of 7.31 au. Wang *et al* [43] had earlier demonstrated that at the FCC phase the lowest energy state of the Fe is a high-spin ferromagnetic state beyond the lattice constant of 6.8 au and that the existence of this state is consistent with the experimental observation that FCC Fe precipitates in Cu–Au alloys (lattice constant = 7.11 au) [44]. Their calculations were done with the LDA functional. Therefore, for FCC Fe at the lattice constants considered for our study, the LDA functional can be used safely. Similar to this case, we see the identical qualitative features in LDA and GGA phonon dispersion results for Fe at the lattice constant of $Pd_{0.96}Fe_{0.04}$ as well, which demonstrates that the Fe is also dynamically unstable at this lattice constant. Consequently, the nearest-neighbor force constants (longitudinal and transverse) as shown in table 1 are much softer than the corresponding ones in the case of pure Pd calculated at the same lattice constants. This is only to be expected as has been discussed before. This softness of the Fe–Fe interactions are expected to remain in the alloys studied as well because of the same lattice structure of the element and the alloy and because of the dependence of longitudinal (stretching) and transverse (bending) force constants on bond distances alone [27]. Therefore, the Fe–Fe interactions as portrayed in the model potential based method are far from reality.

In what follows, we calculate the phonon dispersion curves of these two alloys by the ICPA using the *ab initio*

Fe–Fe and Pd–Pd force constants. As a first approximation, the Fe–Pd force constants are taken to be simple concentration averages of the Fe–Fe and Pd–Pd force constants, as was done in the calculations with the model potentials [24, 25]. The results for $Pd_{96}Fe_4$, calculated with these sets of force constants, are presented in figure 3. The phonon frequencies are obtained from the peaks of the coherent scattering structure factor defined as

$$\langle\langle S_\lambda(\vec{q}, w)\rangle\rangle_{\rm coh} = \sum_{ss'} d_s\, d_{s'} \frac{1}{\pi} {\rm Im}\langle\langle G_\lambda^{ss'}(\vec{q}, w^2)\rangle\rangle \quad (6)$$

where λ is the normal-mode branch index, d_s is the coherent scattering length for the species s and $\langle\langle G_\lambda^{ss'}(\vec{q}, w^2)\rangle\rangle$ is the configuration-averaged spectral function associated with the species pair s, s'. The results show good agreement with experimental results for the major part of the spectrum for the alloy. However, near the zone boundary, spurious splittings in the dispersion curves are observed. This feature of spurious splitting for high values of ζ is observed for the $Pd_{0.9}Fe_{0.1}$ alloy as well. This kind of splitting in dispersion curves is a typical feature of a strong force constant disorder. In [19], the splitting in the dispersion curve for the $Ni_{50}Pt_{50}$ alloy was found to be due to the interplay of the Ni–Ni, Pt–Pt and Ni–Pt force constants whereas in [21], a spurious splitting like the present case was observed in the $Fe_{50}Pd_{50}$ alloy which was due to an overestimation of the Pd–Pd force constants. To understand the sources of the unphysical splittings in our cases, we take recourse in the partial and the average structure factors. In figure 4, we present results for the structure factors along the $[\zeta 00]$ direction and for the longitudinal branch at some selected ζ values. For $Pd_{0.96}Fe_{0.04}$ (figure 4(a)), we observe that the contributions of the Fe pairs to the total structure factors are minuscule and the spectrum is dominated mainly by the Pd pairs. However, the structure factor at the zone boundary has a two-peak structure where the small hump-like peak at a higher frequency is due to substantial contributions from the Fe–Pd pairs. This is the reason behind the existence of the extra longitudinal branches in the dispersion curves. For $Pd_{0.9}Fe_{0.1}$ (figure 4(b)), the peaks in the structure factors are mostly due to the Pd pairs with some contribution from the Fe–Pd pairs for smaller ζ values. However, as one moves towards the zone boundary, a hump starts to show up at higher frequencies, as is seen in the case of the $[0.7, 0, 0]$ longitudinal branch. The hump originates mainly from the Fe–Pd contributions. At the zone boundary, the main peak in the structure factor shifts substantially towards high frequency, producing a split in the dispersion curve. The new peak is now dominated by the Fe–Pd contributions along with contributions from the Pd pairs and Fe pairs. It is interesting to note that, on the lower frequency side where Pd–Pd had dominant contributions, no peak is observed because of the fact that the Fe–Pd contributions have neutralized the Pd–Pd contributions completely. The observations in the structure factor results suggest that, for high ζ values, the Fe–Pd interactions are competing with the Pd–Pd interactions producing the anomalous new branch in the phonon spectrum. That the Fe–Pd interactions are as strong as the Pd–Pd interactions can be understood from the force constants provided in table 1. We can therefore conclude that

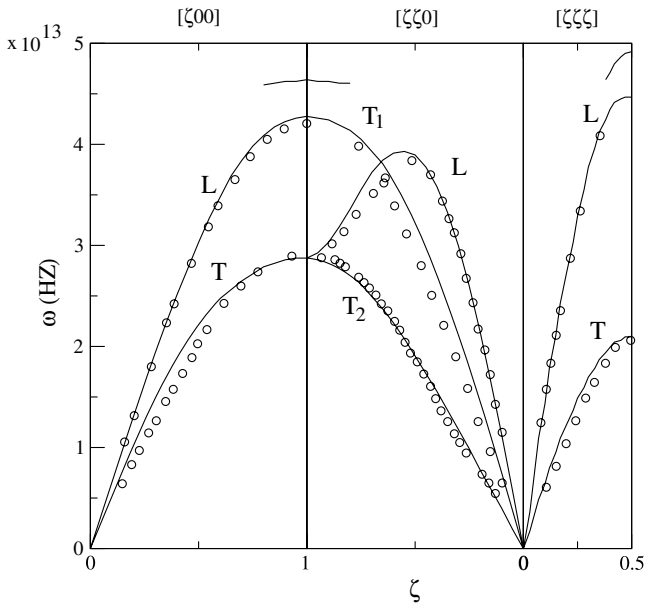

Figure 3. Dispersion curves for $Pd_{0.96}Fe_{0.04}$ calculated by the ICPA. The Fe–Pd force constants are the concentration-averaged ones. The circles are the experimental points.

the Fe–Pd interactions calculated from simple concentration averages of the Fe–Fe and Pd–Pd interactions do not provide a correct picture of the microscopic interactions.

In our endeavor to model the inter-atomic interactions correctly with the help of the *ab initio* force constants, we next try to model the Fe–Pd force constants making use of the following intuitive argument: the basic assumption on which we calculated the Fe–Fe and Pd–Pd force constants at the alloy lattice constants was that the inter-atomic longitudinal and transverse force constants are dependent upon bond distances alone. In the same spirit, the Fe–Pd force constants can, therefore, not be of nearly the same magnitude as the Pd–Pd ones. This intuitive argument is based upon the fact that, in both the alloys considered here, the Fe concentration is very low; therefore in the sample the Pd atoms would find themselves mostly surrounded by Pd atoms, making the average bond distances of Fe–Pd larger than that of Pd–Pd, resulting in the softening of the Fe–Pd interactions in comparison to the Pd–Pd ones.

Based on this intuitive argument, we now reduce the Fe–Pd force constants from the concentration-averaged values, keeping the Fe–Fe and Pd–Pd ones intact. The anomalies in the phonon spectrum completely disappear by a 20% reduction of the Fe–Pd force constants from the concentration-averaged values. In figures 5 and 6 we present the dispersion curves calculated by the ICPA using these new sets of force constants for $Pd_{0.96}Fe_{0.04}$ and $Pd_{0.9}Fe_{0.1}$, respectively. We observe substantially good agreement between the ICPA results and the experimental results for both cases. Corresponding structure factors for [100] longitudinal branches are shown in figures 7 and 8, respectively. Unlike the previous structure factors (figure 4), no dual peak structures appear in these cases. For both alloys, the Fe–Pd contributions are significantly weaker

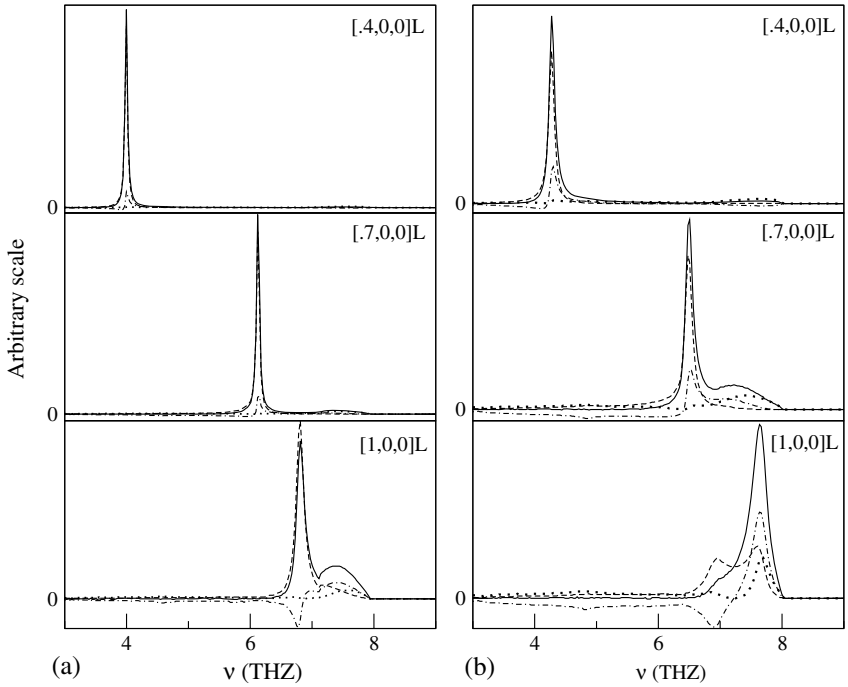

Figure 4. Partial and total structure factors calculated by the ICPA for various ζ values in the $[\zeta, 0,0]$ direction in (a) $Pd_{0.96}Fe_{0.04}$ and (b) $Pd_{0.9}Fe_{0.1}$ using the concentration-averaged Fe–Pd force constants. The solid lines are the total contributions, the dotted lines are the Fe–Fe contributions, the long-dashed lines are the Pd–Pd contributions and the dotted–dashed lines are the Fe–Pd contributions. All the curves are for longitudinal modes.

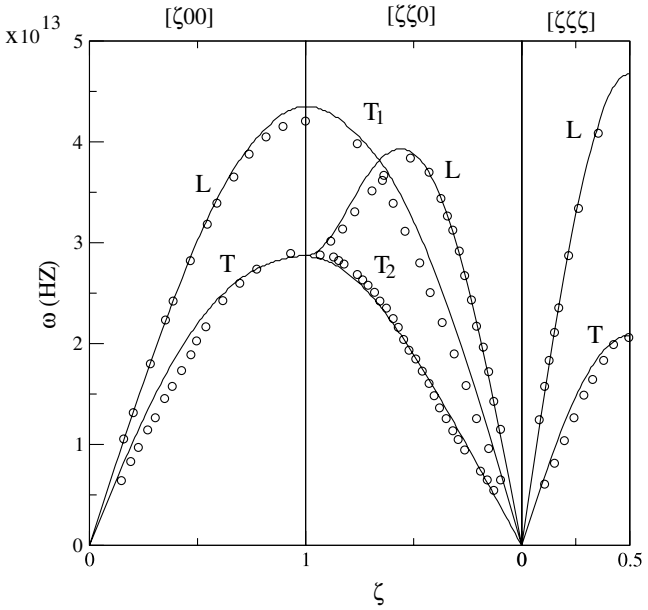

Figure 5. Dispersion curves for $Pd_{0.96}Fe_{0.04}$ with 20% reduced Fe–Pd force constants obtained from the ICPA calculations. The circles are the experimental points.

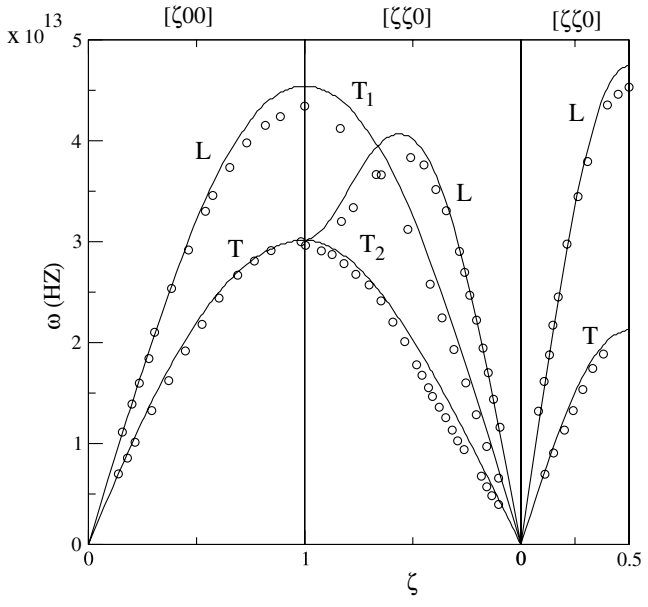

Figure 6. Dispersion curves for $Pd_{0.9}Fe_{0.1}$ with 20% reduced Fe–Pd force constants obtained from the ICPA calculations. The circles are the experimental points.

than the Pd–Pd ones and, at the zone boundary, the Fe–Pd contributions only add more weight to the single peak dominated by the Pd–Pd contributions. The extra peaks which were observed with the concentration-averaged Fe–Pd force constants are now shifted to the lower frequencies and merge with the main peak.

Finally, we calculate the elastic constants in these alloys from the slopes of the phonon dispersion curves in order to check the accuracy and the quality of the phonon frequencies obtained by the modeling strategy adopted here. The results are given in table 2. Results obtained from the model potential calculations [24] and the experiments [23] are also presented

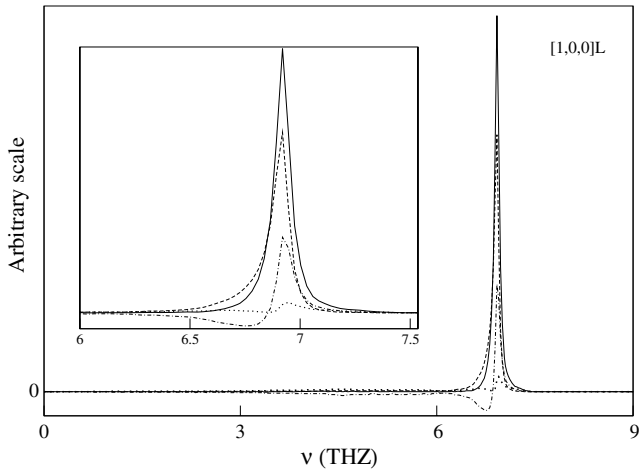

Figure 7. Partial and total structure factors calculated in the ICPA with 20% reduced Fe–Pd force constants for $\zeta = 1$ in the $[\zeta, 0, 0]$ direction in $Pd_{0.96}Fe_{0.04}$. The solid lines are the total contribution, the dotted lines are the Fe–Fe contributions, the long-dashed lines are the Pd–Pd contributions and the dotted–dashed lines are the Fe–Pd contributions. All the curves are for longitudinal modes. The inset shows the contributions from various pairs near the peak.

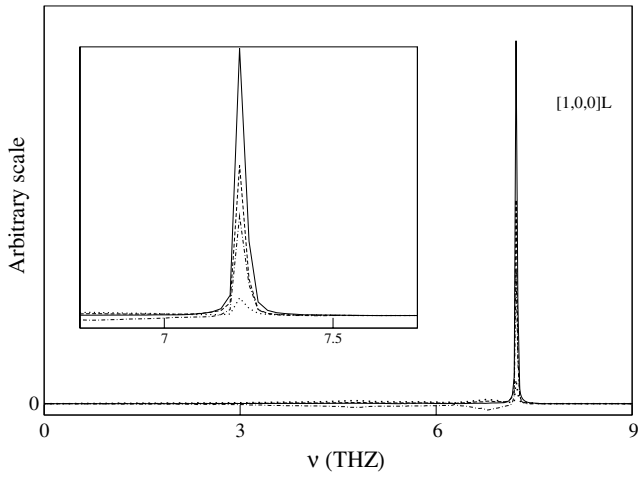

Figure 8. Partial and total structure factors calculated in the ICPA with 20% reduced Fe–Pd force constants for $\zeta = 1$ in the $[\zeta,0,0]$ direction in $Pd_{0.9}Fe_{0.1}$. The solid lines are the total contribution, the dotted lines are the Fe–Fe contributions, the long-dashed lines are the Pd–Pd contributions and the dotted–dashed lines are the Fe–Pd contributions. All the curves are for longitudinal modes. The inset shows the contributions from various pairs near the peak.

for comparison. We observe an overall better agreement of our results with the experimental values than those of the model potential approach. The only significant discrepancy is observed for C_{44} in the case of $Pd_{0.96}Fe_{0.04}$. The average deviation between our results and the experimental ones is about 16%, indicating reasonably good agreement.

5. Conclusions

This paper provides a novel approach to understand the influence of inter-atomic interactions between various pairs of species in a random binary alloy on the lattice dynamics of such systems both qualitatively and quantitatively using Pd_xFe_{1-x} alloys as an example case. The modeling of inter-atomic interactions was based upon the results of *ab initio* calculations and the intuitive argument about dependence of stretching and bending force constants on bond lengths. This strategy incorporated the important electronic structure effects which influence the interplay of forces at the microscopic level and thus provided a realistic and accurate picture which was absent in the approach based upon construction of model potentials. The ICPA, on the other hand, performed the configuration averaging in a self-consistent way taking into account the disorder fluctuations in both mass and force constants. These issues were not addressed in the model potential approach and hence modeling the random alloy by a mean crystal-like one could not provide a realistic picture of disordered fluctuations producing significant differences with the experimental results which can only get exaggerated for a system with stronger mass and force constant disorder like NiPt. Our methodology, a combination of an accurate *ab initio* electronic structure tool and an efficient self-consistent method for configuration averaging, on the other hand, was able to systematically investigate the influences of the force constant fluctuations on the phonon spectrum and therefore understand the microscopic origin of the lattice dynamics in Pd_xFe_{1-x} alloys. The calculated phonon frequencies and the elastic constants agreed very well with the experiments, thus justifying the modeling strategy adopted. This combination of *ab initio* methods, the modeling strategy for force constants adopted here and the ICPA method can, therefore, act as an accurate and efficient tool to study the phonons and related properties for disordered alloys.

Table 2. Computed elastic constants (in units of Mbar) for Pd_xFe_{1-x}.

	$Pd_{0.96}Fe_{0.04}$			$Pd_{0.9}Fe_{0.1}$		
	Theo. (our calc.)	Theo. [24]	Expt. [23]	Theo. (our calc.)	Theo. [24]	Expt. [23]
C_{11}	1.97	1.716	2.3	2.24	1.724	2.29
C_{12}	1.25	1.273	1.53	1.41	1.292	1.65
C_{44}	1.26	1.015	0.78	1.12	1.004	0.86

Acknowledgment

One of the authors (BD) would like to acknowledge CSIR, India for financial support under grant-F. No. 09/731(0049)/2007-EMR-I.

References

[1] Bruesch P 1982 *Phonon, Theory and Experiment* (New York: Springer)
[2] Bogdanoff P D, Fultz B and Rosenkranz S 1999 *Phys. Rev.* B **60** 3976
[3] Fultz B, Anthony L, Robertson J L, Nicklow R M, Spooner S and Mostoller M 1995 *Phys. Rev.* B **52** 3280

[4] Swan-Wood T L, Delaire O and Fultz B 2005 *Phys. Rev.* B **72** 024305
[5] Mehaddene T *et al* 2004 *Phys. Rev.* B **69** 024304
[6] Mozer B, Otnes K and Myers V W 1962 *Phys. Rev. Lett.* **8** 278
Mozer B, Otnes K and Thaper C 1966 *Phys. Rev.* **152** 535
Svensson E C, Brockhouse B N and Rowe J M 1965 *Solid State Commun.* **3** 245
Svensson E C and Brockhouse B N 1967 *Phys. Rev. Lett.* **18** 858
Smith H G and Wilkinson M K 1968 *Phys. Rev. Lett.* **20** 1245
Nicklow R M, Vijayraghavan P R, Smith H G and Wilkinson M K 1968 *Neutron Inelastic Scattering* vol I (Vienna: IAEA) p 47
[7] Cunnigham R M, Muhlestein L D, Shaw W M and Tompson C W 1970 *Phys. Rev.* B **2** 4864
Wakabayashi N, Nicklow R M and Smith H G 1971 *Phys. Rev.* B **4** 2558
Svensson E C and Kamitakahara W A 1971 *Can. J. Phys.* **49** 2291
Wakabayashi N 1973 *Phys. Rev.* B **8** 6015
Brockhouse B N and Nicklow R M 1973 *Bull. Am. Phys. Soc.* **18** 112
Zinken A, Buchenau U, Fenzel H J and Schober H R 1977 *Solid State Commun.* **13** 495
[8] Kamitakahara W A and Brockhouse B N 1974 *Phys. Rev.* B **10** 1200
[9] Tsunoda Y, Kunitomi N, Wakabayashi N, Nicklow R M and Smith H G 1979 *Phys. Rev.* B **19** 2876
[10] Nicklow R M 1983 *Methods of Experimental Physics* vol 23 (New York: Academic) p 172
[11] Taylor D W 1967 *Phys. Rev.* **156** 1017
[12] Blackman J A, Esterling D M and Berk N F 1971 *Phys. Rev.* B **4** 2412
[13] Shiba H 1971 *Prog. Theor. Phys.* **46** 77
[14] Kaplan T and Mostoller M 1974 *Phys. Rev.* B **9** 1783
[15] Takeno S 1968 *Prog. Theor. Phys.* **40** 942
[16] Nickel B G and Butler W 1973 *Phys. Rev. Lett.* **30** 373
[17] Ducastelle F 1974 *J. Phys. C: Solid State Phys.* **7** 1795
[18] Gonis A and Garland J W 1978 *Phys. Rev.* B **18** 3999
[19] Ghosh S, Leath P L and Cohen M H 2002 *Phys. Rev.* B **66** 214206
[20] Ghosh S, Neaton J B, Antons A H, Cohen M H and Leath P L 2004 *Phys. Rev.* B **70** 024206
[21] Alam A, Ghosh S and Mookerjee A 2007 *Phys. Rev.* B **75** 134202
[22] Zarestky J and Stassis C 1987 *Phys. Rev.* B **35** 4500
[23] Maliszewski E, Sosnowski J, Bednarski S, Czachor A and Holas A 1975 *J. Phys. F: Met. Phys.* **5** 1455
[24] Singh N 1990 *Phys. Rev.* B **42** 8882
[25] Akgun I and Ugur G 1995 *Phys. Rev.* B **51** 3458
[26] Upadhyay S C, Prakash D, Sharma D K, Shyam R and Upadhyay J C 1993 *Phys. Status Solidi* b **179** 357
[27] Van De Walle A and Cedar G 2000 *Phys. Rev.* B **61** 5972
[28] Van De Walle A 2000 *PhD Thesis* MIT Cambridge
[29] Liu J Z, Ghosh G, Van De Walle A and Asta M 2007 *Phys. Rev.* B **75** 104117
[30] Baroni S, De Gironcoli S, Dal Corso A and Giannozzi P 2001 *Rev. Mod. Phys.* **73** 515
[31] Hohenberg P and Kohn W 1964 *Phys. Rev.* B **136** 864
[32] Kohn W and Sham L J 1965 *Phys. Rev.* A **140** 1133
[33] Pick R, Cohen M H and Martin R M 1970 *Phys. Rev.* B **1** 910
[34] Hellmann H 1937 *Einfuhrung in die Quantenchemie* (Deuticke: Leipzig)
[35] Feynman R P 1939 *Phys. Rev.* **56** 340
[36] Mookerjee A 1973 *J. Phys. C: Solid State Phys.* **6** 1340
[37] Vanderbilt D 1990 *Phys. Rev.* B **41** 7892
[38] Louie S G, Froyen S and Cohen M L 1982 *Phys. Rev.* B **26** 1738
[39] Perdew J P and Zunger A 1981 *Phys. Rev.* B **23** 5048
[40] Perdew J P, Burke K and Ernzerhof M 1996 *Phys. Rev. Lett.* **77** 3865
[41] Methfessel M and Paxton A T 1989 *Phys. Rev.* B **40** 3616
[42] Moroni E G, Kresse G, Hafner J and Furthmuller J 1997 *Phys. Rev.* B **56** 15629
[43] Wang C S, Klein B M and Krakauer H 1985 *Phys. Rev. Lett.* **54** 1852
[44] Gonser U, Krischel K and Nasu S 1980 *J. Magn. Magn. Mater.* **15–18** 1145